Theory of Partially Drained Piezometer Insertion

By Derek Elsworth,[1] Associate Member, ASCE

Abstract: A theory is presented to evaluate pore pressures developed as a result of insertion of an open-tipped standpipe into a saturated porous medium. An integral method is used whereby the advancing tip is represented as a moving point dislocation. Dimensionless standpipe pressure, $\langle P_D - P_b^i \rangle$, is uniquely controlled in dimensionless time, t_D, by dimensionless penetration rate, U_D/E_D, and the modulus ratio, $E_D(R_2/R_1)^2$. The time lag to pressure buildup is controlled by the magnitude of the ratio of penetration rate, U, to consolidation coefficient, c, as embodied in U_D/E_D. The magnitude of the pressure differential between a closed-tip piezocone and the open standpipe piezometer is exacerbated as the parameter $E_D(R_2/R_1)^2$ is increased, reflecting the volume compressibility of the measuring system. At low relative penetration rates, the steady pore pressure response within the standpipe is subhydrostatic as fluid response is controlled primarily by the in situ hydrostatic pressure distribution with minimal contribution from generated pore pressures. As dimensionless penetration rate U_D/E_D is increased, the standpipe response becomes greater than hydrostatic, indicating the influence of high drivage-induced tip pore pressures on overall behavior.

Introduction

The potential application of field penetrometer testing in the determination of in situ consolidation behavior of soils has been previously recognized (Janbu and Senneset 1974; Wissa et al. 1975; Torstensson 1975; Jones and Van Zyl 1981; Battaglio et al. 1981). Of critical interest in the rational interpretation of data is the mechanism by which pore pressures are generated surrounding the penetrometer tip as a function of the prescribed, assumed, or measured undrained strain field. The strain field may be evaluated from consideration of the kinematic failure mechanisms, either disregarding (Baligh and Scott 1976) or including (Drescher and Kang 1987) self weight, from expanding cavity results in either cohesive (Ladanyi 1963) or cohesive-frictional soils (Carter et al. 1986), or from use of a strain-path-type methodology (Baligh 1985; Tumay et al. 1985; Acar and Tumay 1986). Instantaneous pore pressure distributions may be determined through use of appropriate pore pressure parameters (Skempton 1954; Biot and Willis 1957).

As an alternative to closed-tip piezocones, open-tipped standpipe piezometers may be forced into the soil and the pore pressure changes generated around the tip monitored with time. Rather than directly recording the generated tip pressures, the equilibration process initiated within the open standpipe will enforce both a time lag and a reduction in recorded fluid pressure over the closed-tip piezocone. This behavior is analogous to that reported in the classic time-lag analysis of Gibson (1963). If these data may be recorded during drivage, the hydraulic characteristics of the penetrated medium may be determined from type curve matches. Operationally, pressure heads within

[1]Adjunct Prof., Waterloo Ctr. for Groundwater Res., Univ. of Waterloo, Waterloo, Ontario, Canada N2L 3G1.

Note. Discussion open until November 1, 1990. To extend the closing date one month, a written request must be filed with the ASCE Manager of Journals. The manuscript for this paper was submitted for review and possible publication on May 11, 1989. This paper is part of the *Journal of Geotechnical Engineering*, Vol. 116, No. 6, June, 1990. ©ASCE, ISSN 0733-9410/90/0006-0899/$1.00 + $.15 per page. Paper No. 24723.

the penetrating standpipe may be measured by a single pressure transducer located behind a high air-entry porous filter tip. A theory is presented to account for concurrent pore pressure generation and dissipation mechanisms around the advancing tip of a standpipe piezometer. A solution is based on the theory of a point dislocation moving within a saturated porous medium.

Static Dislocation

Assume that the static piezometer assembly may be represented by a point dislocation located at the origin of the coordinate system $(x,y,z) = (0,0,0)$ as illustrated in Fig. 1. The excess pressure distribution $(p - p_s)$ resulting from an instantaneous point dislocation is given as (Cleary 1977):

$$p - p_s = \frac{cV}{4\pi R^3} \frac{\mu}{k} \frac{\xi^3}{2\sqrt{\pi}} \exp\left(-\frac{\xi^2}{4}\right) \quad \ldots\ldots (1)$$

with

$$\xi = \frac{R}{\sqrt{ct}} \quad \ldots\ldots (2a)$$

and

$$R^2 = x^2 + y^2 + z^2 \quad \ldots\ldots (2b)$$

where p = total fluid pressure; p_s = initial static fluid pressure at the point of interest; c = coefficient of consolidation; μ = fluid dynamic viscosity; k = permeability; t = time following initiation of the dislocation; R = radius of interest; and V = volume introduced as a dislocation. The instantaneous volumetric change is positive for insertion and negative for removal, allowing general mixed volume changes to be accommodated.

For an incremental advance of an open-tipped piezometer, moving at constant velocity U, two effects are manifest. The first is the undrained loading and subsequent drainage of the surrounding medium resulting from the displacement field around the piezometer tip. For a piezometer of effective-tip external area, a, or radius, R_1, as illustrated in Fig. 1, the volume introduced

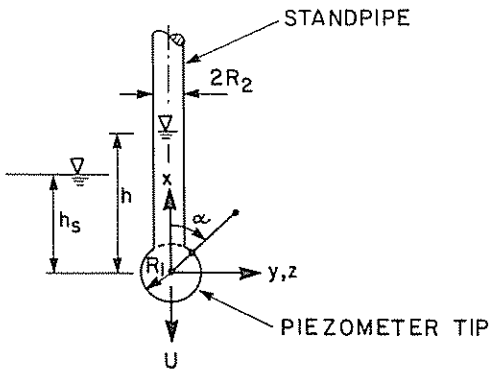

FIG. 1. Schematic of Piezometer Tip and Sandpipe

in time increment $d\tau$ is given by V_1, where

$$V_1 = Uad\tau = U\pi R_1^2 d\tau \quad \ldots\ldots (3)$$

This volume change resulting from mechanical insertion is diminished by a reverse flow into the piezometer under a head differential given as V_2, where

$$V_2 = -A\frac{dh_1}{d\tau}d\tau = -\frac{A}{\gamma_f}\frac{dp_1}{d\tau}d\tau \quad \ldots\ldots (4)$$

where A = the internal cross-sectional area of the standpipe. For a constant internal radius of the standpipe $A = \pi R_2^2$

$$V_2 = -\frac{\pi R_2^2}{\gamma_f}\frac{dp_1}{d\tau}d\tau \quad \ldots\ldots (5)$$

where h_1, p_1 = the head and pressure recorded at $R = R_1$, respectively; and it is assumed that R_1 is sufficiently small that pressure variations over the depth of the spherical surface may be neglected. The total instantaneous volume change is given by $V = V_1 + V_2$ and may be substituted into Eq. 1 to yield

$$p - p_s = \frac{c}{4R^3}\frac{\mu}{k}\frac{\xi^3}{2\sqrt{\pi}}\left(UR_1^2 - \frac{R_2^2}{\gamma_f}\frac{dp_1}{d\tau}\right)\exp\left(-\frac{\xi^2}{4}\right)d\tau \quad \ldots\ldots (6)$$

giving the appropriate pressure response. When the tip of the piezometer, of external radius R_1, has a much greater permeability than the surrounding penetrated media, Eq. 6 may be written specifically for the pressure differential measured at an equivalent radius R_1 corresponding to the radius of the piezometer tip. Accordingly, where, $\xi_1 = R_1/\sqrt{ct}$

$$p_1 - p_s = \frac{c}{4R_1^3}\frac{\mu}{k}\frac{\xi_1^3}{2\sqrt{\pi}}\left(UR_1^2 - \frac{R_2^2}{\gamma_f}\frac{dp_1}{d\tau}\right)\exp\left(-\frac{\xi_1^2}{4}\right)d\tau \quad \ldots\ldots (7)$$

If it is assumed that the static pore pressure magnitude, p_s, is constant over the finite height ($2R_1$) of the piezometer tip, Eq. 7 is clearly spherically symmetric. This will not be replicated, however, when the point dislocation is moved at velocity U to represent penetration of the piezometer. Instead, the area-averaged pressure differential, $\langle p_1 - p_s\rangle$, may be evaluated over the surface at radius R_1 such that

$$\langle p_1\rangle = \frac{c}{4R_1^3}\frac{\mu}{k}\frac{\xi_1^3}{2\sqrt{\pi}}\frac{1}{2}\int_0^{\pi}\left[UR_1^2 - \frac{R_2^2}{\gamma_f}\frac{dp(x)_1}{d\tau}\right]\exp\left(-\frac{\xi_1^2}{4}\right)\sin\alpha d\alpha d\tau + p_s \quad (8)$$

where $\langle p_1\rangle = 1/2\int_0^{\pi} p_1(x)\sin\alpha d\alpha$ and α is the angle subtended from the positive x-axis as illustrated in Fig. 1.

Moving Dislocation

The fluid-tapped static dislocation of Eq. 8 may be integrated in time and space, as illustrated in Fig. 2, to represent the advance of an open-tipped piezometer. A coordinate system fixed to the center of the piezometer tip is chosen that moves in the medium at velocity $-U$. In moving, the dislocation leaves a remnant void of volume, $Vd\tau$, along the travel path representing the

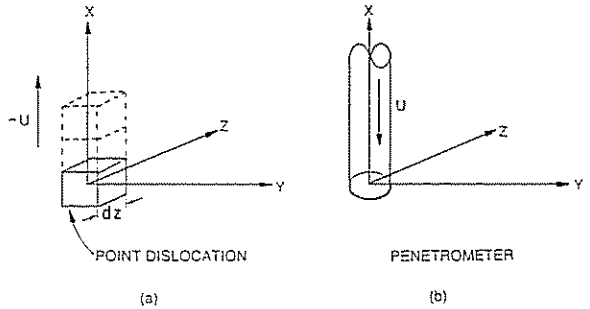

FIG. 2. (*a*) Point Dislocation within Saturated Porous Medium Moving at Velocity, U; (*b*) Analogy with Penetrometer Moving at Velocity, U

volume displaced by the constant radius piezometer casing.

For all times $t \geq 0^+$, a point dislocation is introduced at the origin at rate V per unit time and the surrounding medium moves at velocity U relative to the coordinate system. The position of a point in the surrounding medium located at (x, y, z) at current time t would have been $[x - U(t - \tau), y, z]$ at time τ. Under this condition, Eq. 8 may be rewritten as

$$\langle p_1 \rangle = \frac{c}{4\bar{R}_1^3} \frac{\mu}{k} \frac{\xi_2^3}{2\sqrt{\pi}} \frac{1}{2} \int_0^{\pi} \left[UR_1^2 - \frac{R_2^2}{\gamma_f} \frac{dp_1(x)}{d\tau} \right] \exp\left(-\frac{\xi_2^2}{4}\right) \sin \alpha d\alpha d\tau + p_s \qquad (9)$$

where

$$\xi_2 = \frac{\bar{R}_1}{\sqrt{c(t - \tau)}} \qquad (10a)$$

$$\bar{R}_1^2 = [x - U(t - \tau)]^2 + y^2 + z^2 \qquad (10b)$$

to give the pressure differential at time t due to the point dislocation, $Vd\tau$, introduced at time τ. The integrated effect is directly evident from Eq. 9 as

$$\langle p_1 \rangle = \int_0^t \frac{c}{4\bar{R}_1^3} \frac{\mu}{k} \frac{\xi_2^3}{2\sqrt{\pi}} \frac{1}{2} \int_0^{\pi} \left[UR_1^2 - \frac{R_2^2}{\gamma_f} \frac{dp_1(x)}{d\tau} \right]$$

$$\exp\left(-\frac{\xi_2^2}{4}\right) \sin \alpha d\alpha d\tau + p_s \qquad (11)$$

where the substitution, $\eta = R_1/2[c(t - \tau)]^{1/2}$, may be applied to yield

$$\langle p_1 - p_0 \rangle = \frac{1}{2\sqrt{\pi} R_1} \frac{\mu}{k} \int_{R_1/2(ct)^{1/2}}^{\infty} \frac{1}{2} \int_0^{\pi} \left[UR_1^2 - \frac{R_2^2}{\gamma_f} \frac{dp_1(x)}{d\tau} \right]$$

$$\exp\left[\frac{Ux}{2c} - \eta^2 - \left(\frac{UR_1}{4c\eta}\right)^2\right] \sin \alpha d\alpha d\eta + \langle p_s - p_0 \rangle \qquad (12)$$

where $x = R_1 \cos \alpha$; and $p_0 =$ the equilibrated tip pressure prior to the initiation of penetration assumed constant over the height of the open piezometer bulb. A set of dimensionless parameters may further be defined to

identify the response of the system where behavior during penetration is uniquely defined in terms of

$$P_D = \frac{\langle p_1 - p_0 \rangle}{\gamma_f R_1} \quad (13a)$$

$$P_D^s = \frac{\langle p_s - p_0 \rangle}{\gamma_f R_1} \quad (13b)$$

$$t_D = \frac{4ct}{R_1^2}; \qquad \tau_D = \frac{4c\tau}{R_1^2} \quad (14)$$

$$U_D = \frac{U}{\gamma_f} \frac{\mu}{k} \quad (15)$$

$$E_D = \frac{c}{\gamma_f R_1} \frac{\mu}{k} = \frac{2G(1-\nu)}{(1-2\nu)} \frac{1}{\gamma_f R_1} \quad (16)$$

$$x_D = \frac{x}{R_1} \quad (17)$$

and R_2/R_1 where P_D = dimensionless pressure; t_D = dimensionless time; U_D = dimensionless penetration rate; E_D = dimensionless modulus of deformation; G = shear modulus; and ν = Poisson's ratio. For a hydrostatic groundwater system, $\langle p_s - p_0 \rangle = Ut\gamma_f$ and

$$P_D^s = \frac{U_D t_D}{4E_D} \quad (18)$$

In dimensionless form, Eq. 12 may be represented as

$$P_D + \frac{2E_D}{\sqrt{\pi}} \left(\frac{R_2}{R_1}\right)^2 \int_{(t_D)^{-1/2}}^{\infty} \frac{dP_D}{d\tau_D} \frac{1}{2} \int_0^{\pi} f_1\left(\frac{U_D}{E_D}, \alpha, \eta\right) \sin \alpha d\alpha d\eta$$

$$= \frac{U_D}{2\sqrt{\pi}} \int_{(t_D)^{-1/2}}^{\infty} \frac{1}{2} \int_0^{\pi} f_1\left(\frac{U_D}{E_D}, \alpha, \eta\right) \sin \alpha d\alpha d\eta + \frac{U_D t_D}{4E_D} \quad (19)$$

where

$$f_1\left(\frac{U_D}{E_D}, \alpha, \eta\right) = \exp\left[\frac{U_D \cos \alpha}{2E_D} - \eta^2 - \left(\frac{U_D}{4E_D \eta}\right)^2\right] \quad (20)$$

The integral expression may be evaluated numerically where a finite differential is substituted in time as

$$\left(\frac{dP_D}{d\tau_D}\right)^n \equiv \frac{\Delta P_D^n}{\Delta \tau_D^n} = \frac{(P_D^n - P_D^{n-1})}{(t_D^n - t_D^{n-1})} \quad (21)$$

for time step n. Expanding Eq. 19 as a series allows the development of dimensionless pressure to be determined through the current time level, t^{l+1}, where the integrals are represented as

$$I^n = \int_{a_2}^{a_1} \frac{1}{2} \int_0^{\pi} f_1\left(\frac{U_D}{E_D}, \alpha, \eta\right) \sin \alpha d\alpha d\eta \quad (22)$$

with

$$a_1 = \frac{R_1}{2(ct^{n-1})^{1/2}} = (t_D^{n-1})^{-1/2} \quad \ldots\ldots (23a)$$

$$a_2 = \frac{R_1}{2(ct^{n})^{1/2}} = (t_D^{n})^{-1/2} \quad \ldots\ldots (23b)$$

and

$$P_D^{l+1} + \frac{2E_D}{\sqrt{\pi}}\left(\frac{R_2}{R_1}\right)^2\left(\frac{\Delta P_D^1}{\Delta\tau_D^1} I^1 + \frac{\Delta P_D^2}{\Delta\tau_D^2} I^2 + \frac{\Delta P_D^3}{\Delta\tau_D^3} I^3 + \ldots + \frac{\Delta P_D^{l+1}}{\Delta\tau_D^{l+1}} I^{l+1}\right)$$

$$= \frac{U_D}{2\sqrt{\pi}} \int_{(t_D^{l+1})^{-1/2}}^{\infty} \frac{1}{2} \int_0^{\pi} f_1\left(\frac{U_D}{E_D}, \alpha, \eta\right) \sin\alpha d\alpha d\eta + \frac{U_D t_D^{l+1}}{4E_D} \quad \ldots\ldots (24)$$

or, finally

$$\left[1 + \frac{2E_D}{\sqrt{\pi}}\left(\frac{R_2}{R_1}\right)^2 \frac{1}{\Delta\tau_D^{l+1}} I^{l+1}\right] P_D^{l+1} = \frac{2E_D}{\sqrt{\pi}}\left(\frac{R_2}{R_1}\right)^2\left(\frac{P_D^l}{\Delta\tau_D^{l+1}} I^{l+1} - \sum_{n=0}^{l} \frac{\Delta P_D^n}{\Delta\tau_D^n} I^n\right)$$

$$+ \frac{U_D}{2\sqrt{\pi}} \int_{(t_D^{l+1})^{-1/2}}^{\infty} \frac{1}{2} \int_0^{\pi} f_1\left(\frac{U_D}{E_D}, \alpha, \eta\right) \sin\alpha d\alpha d\eta + \frac{U_D t_D^{l+1}}{4E_D} \quad \ldots\ldots (25)$$

enabling P_D^{l+1} to be determined directly from knowledge of the initial condition $P_D = 0$ for $t_D < 0$.

Pore Pressure Response

Eq. 25 may be solved directly to determine the pore pressure response of the system to penetration. For soils, reasonable magnitudes of the dimensionless modulus E_D would be in the range of 10^0–10^6, allowing behavior to be documented with dimensionless time for a variety of penetration rates, U_D. It is instructive to view the penetration behavior under two simplifying conditions prior to observing the fully coupled behavior. The simplifications alternately examine the influence of enforcing a zero in situ pore pressure gradient during penetration (by disregarding the last term of Eq. 25) and alternately assuming that no excess pore pressures are generated during penetration (by setting $V_1 = 0$ in Eq. 3).

Zero Vertical Pore Pressure Gradient

The responses for $E_D(R_2/R_1)^2 = 10^0$, 10^3, and 10^6 are illustrated in Figs. 3(*a*)–3(*c*). When the vertical pore pressure gradient is ignored ($dP_D^s/dt_D = 0$), dimensionless pressure magnitudes are always positive for a full range of penetration rates. This is a direct consequence of the pore fluid pressures generated during drivage being able to dissipate upwards through the shaft of the penetrometer. As the rate U_D/E_D increases, the magnitude of excess pore pressures decrease. This will be manifest as either penetration rate, U, or tip radius, R_1, increases or as consolidation coefficient, c, decreases. For a closed-tip penetrometer, the steady pressure distribution is given by $4(P_D - P_D^s)/U_D = 10^0$ corresponding to the upper limit of the vertical scale of Figs. 3(*a*)–3(*c*). Since the measuring system in the open-tipped penetrometer

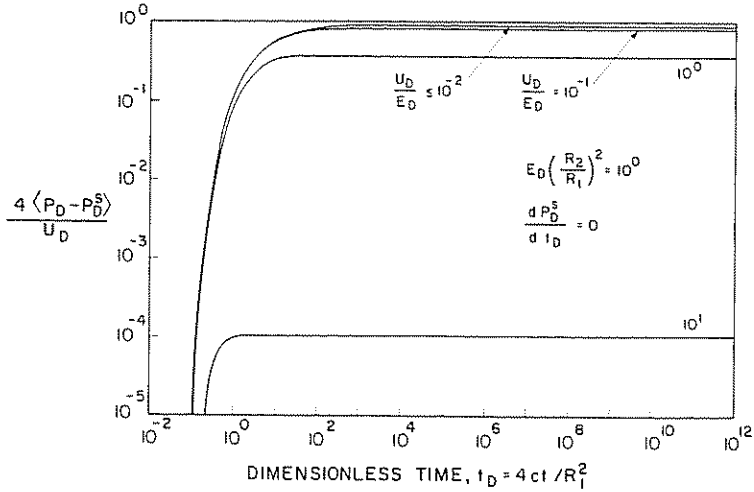

FIG. 3(*a*). Transient Pore Pressure Response at Piezometer Tip for Penetration in Saturated Medium with No Pore Pressure Gradient with Depth: $E_D(R_2/R_1)^2 = 10^0$

has a finite volume, the pressures generated must, in all cases, be lower than for the closed-tip system. As the penetration rate increases, a larger internal volume is produced per unit time in the measuring system, thus exacerbating the influence of pressure lag magnitude in the steady condition.

The magnitudes of steady dimensionless pore pressures are increased with a decrease in the modulus magnitude $E_D(R_2/R_1)^2$ corresponding to a decrease in the volume lag present within the measuring system. The reduction in the

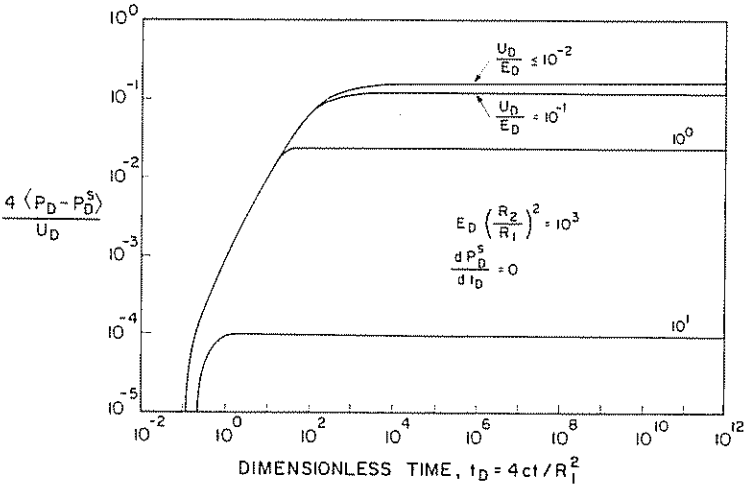

FIG. 3(*b*). Transient Pore Pressure Response at Piezometer Tip for Penetration in Saturated Medium with No Pore Pressure Gradient with Depth: $E_D(R_2/R_1)^2 = 10^3$

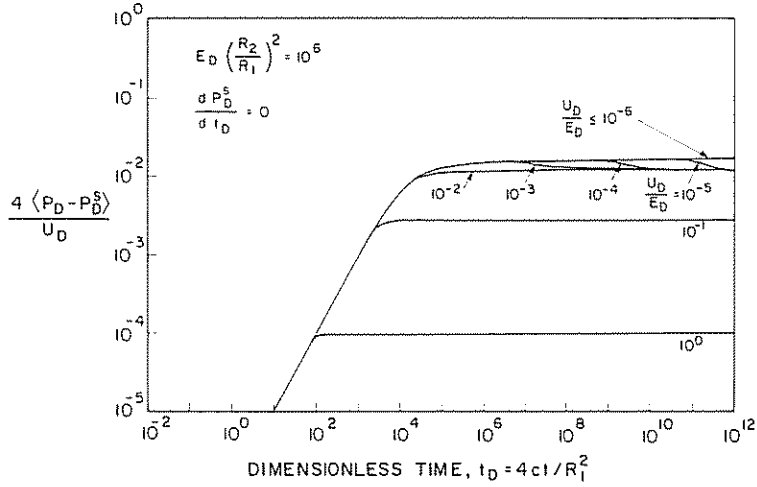

FIG. 3(*c*). Transient Pore Pressure Response at Piezometer Tip for Penetration in Saturated Medium with No Pore Pressure Gradient with Depth: $E_D(R_2/R_1)^2 = 10^6$

volume of the measuring system may be viewed as an overall reduction of system flexibility, in the elastic context. As the internal radius R_2 decreases, the response time is accelerated and the time lag associated with the instrument is decreased. Pore pressures become asymptotic to the closed-tip response as $E_D(R_2/R_1)^2$ approaches zero.

As dimensionless penetration rate, U_D/E_D, is increased beyond 10^2, no appreciable pressure generation is recorded. This situation corresponds to small magnitudes of consolidation coefficient, c, or small component moduli, E, of the saturated material. Physically, the low fluid pressures generated are a direct consequence of the low stiffness of the saturated material requiring application of little force to completely develop the required volume of dislocation. Conversely, for small penetration rate magnitudes with $U_D/E_D \leq 10^{-1}$, a threshold behavior is approached in the steady condition. Notably, as a result of the finite volume of the measuring system, the threshold steady response is less than that for a closed penetrometer.

Zero Excess Pressure Generation

When the effect of the in situ hydrostatic pore pressure gradient is reinstated, the equilibration rate of a moving piezometer may be examined in the absence of pore pressure generation by setting $V_1 = 0$ in Eq. 3. The results of this exercise are illustrated in Figs. 4(*a*)–4(*c*) for the range of parameters $E_D(R_2/R_1)^2 = 10^0, 10^3, 10^6$. Since no excess pressures are generated, the magnitudes of the dimensionless pore pressure ratio $4\langle P_D - P_D^s \rangle / U_D$ are always negative, representing absolute pressures below hydrostatic.

Dimensionless steady pore pressure magnitudes approach hydrostatic with an increase in dimensionless penetration rate U_D/E_D, corresponding to an increase in real penetration rate U, or a decrease in deformation modulus, E, or permeability, k. As the deformation modulus decreases, the volume of fluid available under a small change in fluid pressure is proportionately

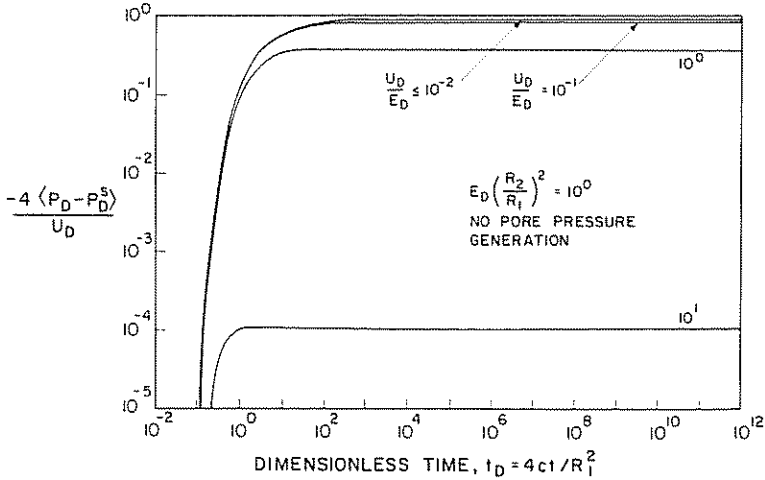

FIG. 4(*a*). Transient Pore Pressure Response at Piezometer Tip for Penetration in Saturated Medium with No Pore Pressure Generation. Piezometer Records Equilibration of In Situ Hydrostatic Pore Pressure Gradient: $E_D(R_2/R_1)^2 = 10^0$

increased to satisfy the requirements of the measuring system. The morphology of the pressure bulb induced around the piezometer tip by reverse flow into the standpipe becomes elongated with increased penetration rate, U_D/E_D. The steep pressure gradients generated at the tip are sufficient to rapidly satisfy the requirements of the measuring system and result in hy-

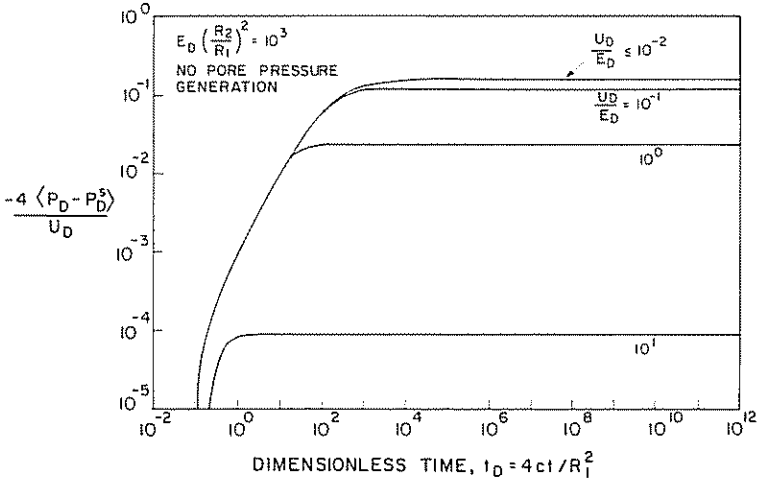

FIG. 4(*b*). Transient Pore Pressure Response at Piezometer Tip for Penetration in Saturated Medium with No Pore Pressure Generation. Piezometer Records Equilibration of In Situ Hydrostatic Pore Pressure Gradient: $E_D(R_2/R_1)^2 = 10^3$

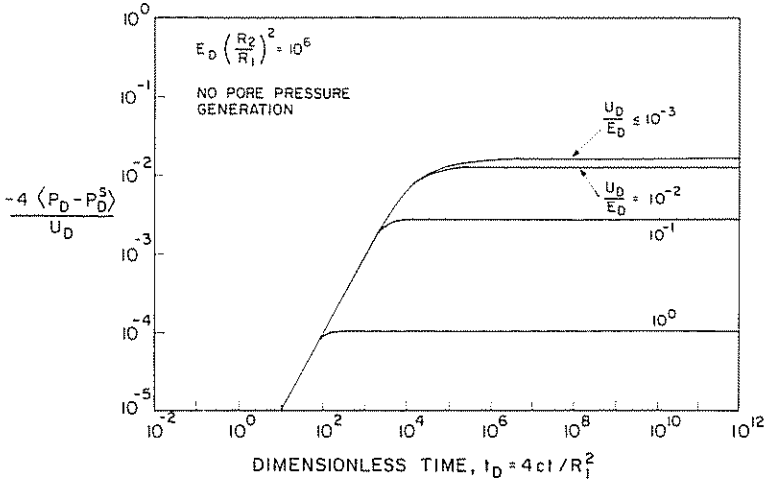

FIG. 4(c). Transient Pore Pressure Response at Piezometer Tip for Penetration in Saturated Medium with No Pore Pressure Generation. Piezometer Records Equilibration of In Situ Hydrostatic Pore Pressure Gradient: $E_D(R_2/R_1)^2 = 10^6$

drostatic dimensionless pressures being maintained in the instrument for large U_D/E_D.

Of these results it appears reasonable that the equilibrium water level in the standpipe approaches hydrostatic as modulus decreases, however, results are counterintuitive when this behavior is also returned where penetration rate, U, increases or permeability, k, decreases. The opposite would be expected. This artifact is exacerbated through the use of the dimensionless quantity $4\langle P_D - P_D^s\rangle/U_D$ that is proportional to k and inversely proportional to U.

As the modulus ratio, $E_D(R_2/R_1)^2$, is decreased, the magnitude of the steady pore pressures below hydrostatic are correspondingly increased and response time is accelerated. A reduction in the cross-sectional area of the standpipe reduces both the resulting time lag and the effective volume compressibility of the measuring system. For dimensionless penetration rate magnitudes $U_D/E_D \leq 10^{-1}$, a threshold behavior is approached in dimensionless time. At this threshold, the equilibrium pressure approaches a steady state where fluid storage in the saturated medium has essentially no effect corresponding to a large deformation modulus, E, or large permeability, k. In this regime, the absolute pore pressure magnitude, $\langle p - p_s\rangle$, will be increased in direct proportion to any increase in the real penetration rate, U. When the stiffness of the penetrated medium is decreased, the magnitude of the dimensionless penetration rate, U_D/E_D, required to reach a threshold behavior increases.

For $U_D/E_D \geq 10^2$, no appreciable magnitude of pore water pressure differential is apparent, suggesting that the corresponding low coefficient of consolidation, c, supplies a sufficient volume of pore fluid from storage to directly balance insertion of the open penetrometer.

Coupled Response

Where the influence of a hydrostatic pore pressure gradient and pore pres-

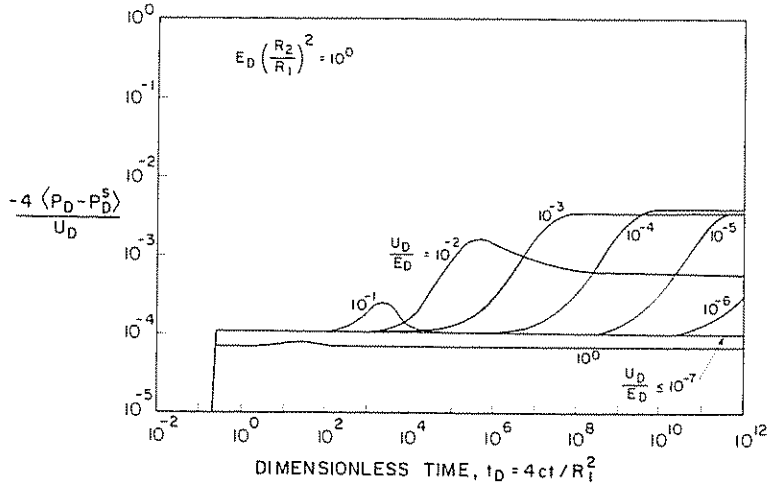

FIG. 5(*a*). Transient Pore Pressure Response at Piezometer Tip for Penetration in Saturated Medium with Pore Pressure Generation and In Situ Hydrostatic Pore Pressure Gradient: $E_D(R_2/R_1)^2 = 10^0$

sure generation effects at the tip of the advancing piezometer are combined, as embodied in Eq. 25, the resulting response is illustrated in Figs. 5(*a*)–5(*c*). For very small magnitudes of dimensionless penetration rate, ($U_D/E_D \le 10^{-3}$), the dimensionless pressure response is always negative, or less than hydrostatic. The resulting steady pore pressure magnitudes for small U_D/E_D

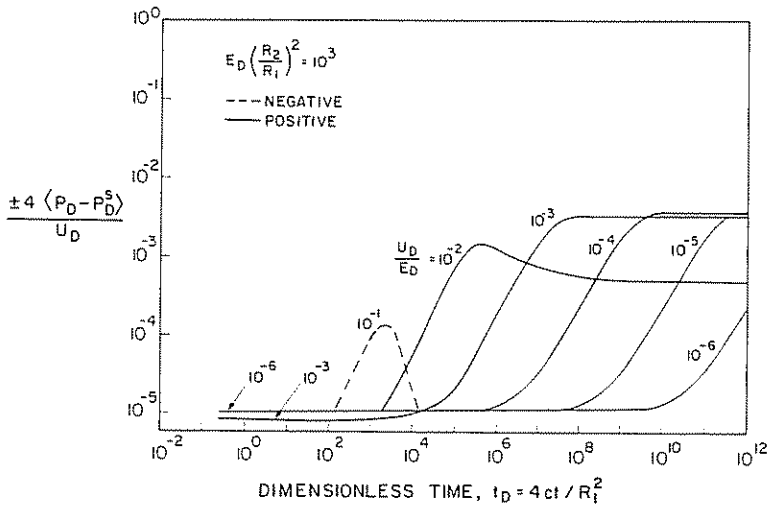

FIG. 5(*b*). Transient Pore Pressure Response at Piezometer Tip for Penetration in Saturated Medium with Pore Pressure Generation and In Situ Hydrostatic Pore Pressure Gradient: $E_D(R_2/R_1)^2 = 10^3$

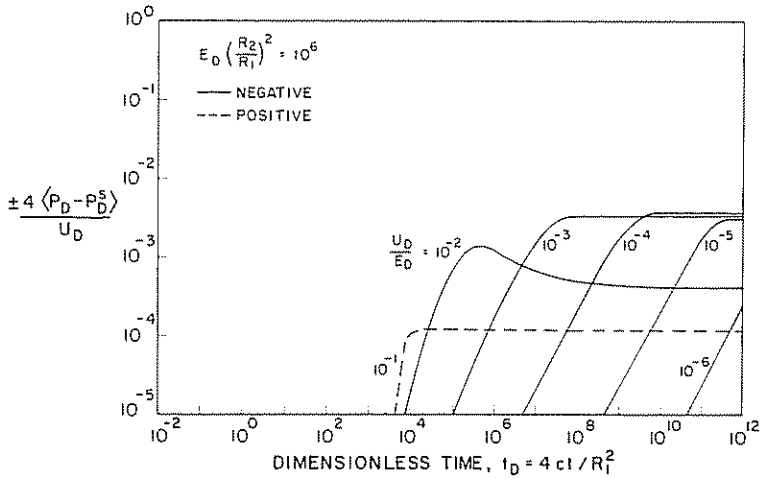

FIG. 5(*c*). Transient Pore Pressure Response at Piezometer Tip for Penetration in Saturated Medium with Pore Pressure Generation and In Situ Hydrostatic Pore Pressure Gradient: $E_D(R_2/R_1)^2 = 10^6$

remain relatively constant with variation in dimensionless modulus, $E_D(R_2/R_1)^2$, recording $4\langle P_D - P_D^s\rangle/U_D \cong -3.8 \times 10^{-3}$ as illustrated in Figs. 5(*a*)–5(*c*). As the penetration rate magnitude is increased, the steady pressure differential magnitudes become briefly positive and then asymptotic to zero. As the penetration rate, U_D/E_D, is decreased, the magnitude of time lag becomes successively more pronounced.

The transient response is a complex combination of the behaviors discretely identified that result jointly from pore pressure generation at the tip and the influence of the in situ pore pressure gradient. For transient behavior, a threshold pore pressure is established at early times as a result of the natural in situ pressure gradient. This threshold magnitude is small (on the order of 10^{-4}) but increases with a decrease in the modulus ratio, $E_D(R_2/R_1)^2$. This dominates response before the influence of generated pore pressures are mobilized and halt the monotonic increase in pore pressure differential below hydrostatic. Then, as the piezometer is advanced further against the in situ hydrostatic gradient, backflow against the natural pore pressure regime further dominates, resulting in the establishment of a steady subhydrostatic pore pressure differential. The magnitude of this steady pressure differential is closer to the null pressure condition than is exhibited, where pore pressure generation at the tip is ignored. This identifies the mutual interference of the two effects in determining the ultimate steady pressure magnitude. As the penetration rate is decreased, the onset of the steady condition is deferred later in dimensionless time as the time taken for in situ pressures to develop becomes successively protracted.

The true behavior is revealed more definitively where dimensionless pressure, $\langle P_D - P_D^s\rangle$, is recorded rather than pressure ratio, $4\langle P_D - P_D^s\rangle/U_D$, for the steady condition as illustrated in Fig. 6. At very low magnitudes of dimensionless penetration rate, $(U_D/E_D \leq 10^{-2})$, corresponding to partially

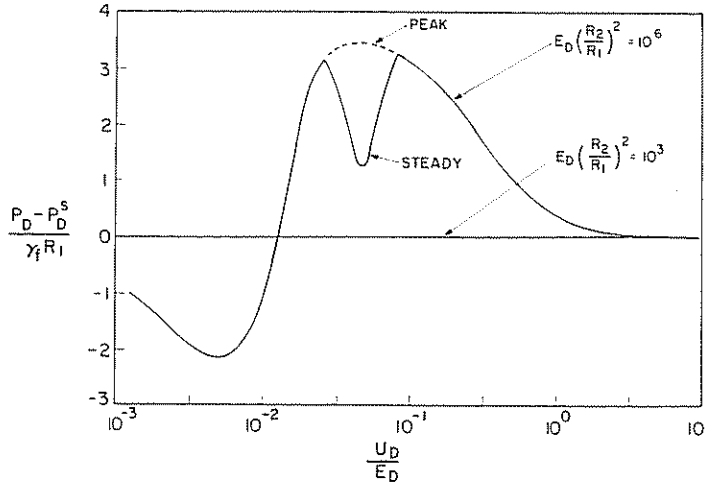

FIG. 6. Steady Pore Pressure Magnitudes Generated Through Penetrometer Advance at Different Dimensionless Penetration Rates, U_D/E_D

drained loading in gravels and sands, the pore pressures remain subhydrostatic. As penetration rate is increased, standpipe pressures become greater than hydrostatic before subsiding as the U_D/E_D ratio is further increased. The changing form of the pressure response, as dimensionless penetration rate, U_D/E_D, is increased, is of particular interest. At extremely low magnitudes of $U_D/E_D(<10^{-3})$, the permeability of the saturated medium is sufficiently high that no significant pore pressure differential, $\langle P_D - P_D^s \rangle$, may develop. As the penetration rate is increased, a subhydrostatic pressure differential is recorded where reduced permeabilities establish an impedance to drainage towards the standpipe. As U_D/E_D is further increased, penetration-generated pore pressures dominate the response as excess standpipe pressures become positive and reach a peak magnitude. Continued increases in U_D/E_D correspond to a further reduction in coefficient of consolidation, c, interpreted as reduced stiffness of the saturated medium. As stiffness is decreased, the force required to introduce a given volumetric dislocation is reduced with the net effect that excess pore pressures become negligibly small. Additionally, at higher penetration rates, pore pressures that are generated remain close to the $y = z = 0$ axis with a resulting rapid dissipation allowing rapid equilibration and ready establishment of null state with $\langle P_D - P_D^s \rangle \rightarrow 0$.

A bifurcation in behavior occurs for magnitudes of dimensionless penetration rate $U_D/E_D \approx 8 \times 10^{-2}$ where the steady tip pressure is lower than a transient peak. The initial peak develops as drivage-induced pore pressures are generated at the tip and ultimately subside as the influence of the in situ pore pressure gradients induce reverse flow into the instrument.

Conclusions

A method is developed to evaluate pore pressure generation and equilibration within an advancing open-tipped piezometer. The following conclu-

sions may be drawn from parametric studies representative of a variety of measuring system flexibilities $E_D(R_2/R_1)^2$.

1. A simplified analysis assuming linear behavior of the individual components is illustrated to yield a complex nonlinear response, as exemplified in Fig. 6, where true interaction between the components is enforced. This emphasizes the complexity of this rudimentary physical system prior to the incorporation of complex material behavior.
2. The pore pressure response appears either subhydrostatic or superhydrostatic during penetration with this state controlled by the dimensionless penetration rate U_D/E_D. This behavior is most directly embodied in Fig. 6, illustrating that at high penetration rates the large penetration-induced pore pressures are readily dissipated into the tip as a result of the restricted size of pressure bulb morphology causing no net pressure increase above hydrostatic. Similarly, at very low penetration rates, the temporal response is sufficiently rapid that no net pressure differential from hydrostatic may be sustained.
3. At intermediate magnitudes of penetration rate, steady pore pressures are superhydrostatic where pore pressure generation effects dominate and subhydrostatic where reverse flow induced by the in situ pore pressure gradient controls the response.
4. Subhydrostatic pore fluid pressures are often encountered during piezocone penetration of silts. It is the volume compressibility of the measuring system, $E_D(R_2/R_1)^2$, that controls the magnitude of the subhydrostatic pore fluid pressures for an open-tipped piezometer. The causal mechanism, however, is the absence or low intensity of penetration generated pore pressures precipitating a time lag for reverse flow into the instrument. Where system flexibilities remain finite in closed-tip piezocone-type instruments, this artifact may explain some of the occurrences of subhydrostatic pore pressures recorded to date.
5. The results from pressure buildup through piezometer insertion may be used to determine in situ parameters only if the appropriate penetration regime may be identified a priori. For example, observing only the results for very low penetration magnitudes ($U_D/E_D \leq 10^{-1}$), the time to the steady condition may be approximated from Figs. 5(*a*)–5(*c*) as $(U_D/E_D)^2 t_D \approx 20$. From this, the magnitude of consolidation coefficient, c, may be uniquely determined when the penetration rate, U, is documented. In an analogous manner, the coefficient of consolidation may be determined from piezocone results where the time to reach a steady pressure distribution is recorded. Operationally, however, this is difficult to determine since the low compressibility of the measuring system results in rapid attainment of equilibrium. The larger system compressibility by the piezometer extends this lag and potentially enables c to be evaluated following the initiation of penetration. Within the low penetration rate range ($U_D/E_D \leq 10^{-3}$) the establishment of a steady pore pressure response may also be utilized to determine in situ permeability magnitudes. Where $4(P_D - P_D^s)/U_D \approx -3.8 \times 10^{-1}$, the magnitude of k/μ may be evaluated uniquely if U_s and $(p - p_s)$ are recorded. Clearly, the most important aspect in applying these methods of data reduction is initially establishing the range U_D/E_D. Once the parameters are determined, the initial estimate range of U_D/E_D may be confirmed.

Acknowledgments

This paper represents partial results of work supported by the Waterloo Centre for Groundwater Research. The source of this funding is gratefully acknowledged.

Appendix I. References

Acar, Y. B., and Tumay, M. T. (1986). "Strain field around cones in steady penetration." *J. Geotech. Engrg. Div.*, ASCE, 112, 207–213.

Baligh, M. M. (1985). "Strain path method." *J. Geotech. Engrg. Div.*, ASCE, 111(9), 1108–1136.

Baligh, M. M., and Scott, R. F. (1976). "Analysis of wedge penetration in clay." Geotechnique, London, England, 26(1), 185–208.

Battaglio, M., et al. (1981). "Piezometer probe test in cohesive deposits." *Proc. Symp. on Cone Penetration Testing and Experience*, ASCE, 264–302.

Biot, M. A., and Willis, D. G. (1957). "The elastic coefficients of the theory of consolidation." *J. Applied Mech.*, 24, 594–601.

Carter, J. P., Booker, J. R., and Yeung, S. K. (1986). "Cavity expansion in cohesive-frictional soils." *Geotechnique*, London, England, 36(3), 349–358.

Cleary, M. P. (1977). "Fundamental solutions for a fluid-saturated porous solid." *Int. J. Solids and Structures*, 13, 785–806.

Drescher, A., and Kang, M. (1987). "Kinematic approach to limit load for steady penetration in rigid-plastic soils." *Geotechnique*, 37(3), London, England, 233–246.

Gibson, R. E. (1963). "An analysis of system flexibility and its effect on time lag in pore-water pressure measurements." *Geotechnique*, London, England, 13, 1–11.

Janbu, N. M., and Senneset, K. (1974). "Effective stress interpretation of in situ static penetration tests." *Proc. European Symp. on Penetration Testing*, Stockholm, Sweden, 1, 181–193.

Jones, G. A., and Van Zyl, D. J. A. (1981). "The piezometer probe—a useful investigation tool." *Proc. 10th ICSMFE*, Stockholm, Sweden, 2, 489–496.

Ladanyi, B. (1963). "Expansion of a cavity in a saturated clay medium." *J. Soil Mech. and Found. Engrg. Div.*, ASCE, 89(4), 127–161.

Rice, J. R., and Cleary, M. P. (1976). "Some basic stress diffusion solutions for fluid-saturated elastic porous media with compressible constituents." *Reviews of Geophysics and Space Physics*, 14(2), 227–241.

Skempton, A. W. (1954). "The pore-pressure coefficients A and B." *Geotechnique*, London, England, 4, 143–147.

Torstensson, B. A. (1975). "Pore pressure sounding instrument." *Proc. ASCE Specialty Conference on In Situ Measurement in Soil Properties*, ASCE, 2, 48–54.

Tumay, M. T., et al. (1985). "Flow field around cone in steady penetration." *J. Geotech. Engrg. Div.*, ASCE, 111, 198–204.

Wissa, A. E. Z., Martin, R. T., and Garlanger, J. E. (1975). "The piezometer probe." *Proc. ASCE Specialty Conference on In Situ Measurement of Soil Properties*, ASCE, 1, 536–545.

Appendix II. Notation

The following symbols are used in this paper:

A = internal cross-sectional area of standpipe;
a = effective tip cross-sectional area;
a_1, a_2 = limits of integration;
c = coefficient of consolidation of porous medium;
E_D = dimensionless deformation modulus;
f_1 = integral parameter;
h_1 = hydraulic head within piezometer;
h_s = static in situ hydraulic head;
G = shear modulus;
I^{l+1} = integral evaluated at time level $l + 1$;

k = permeability of porous medium;
l = time increment counter as superscript;
P_D, P_D^s = dimensionless tip pressure, dimensionless in situ pressure;
p = total pore fluid pressure;
p_s = initial in situ pore fluid pressure;
p_0 = equilibrium tip pressure prior to initiation of penetration;
$p_1(x)$ = pore fluid pressure at radius R_1 and location $x = R_1 \cos \alpha$;
$\langle p_1 \rangle$ = aggregate tip pressure;
R, R_1, R_2 = radius of interest $R^2 = x^2 + y^2 + z^2$, tip radius, standpipe radius;
t = time following initiation of penetration;
t_D = dimensionless time;
U = piezometer penetration rate;
V = dislocation volume;
x, y, z = Cartesian coordinates;
x_D = dimensionless coordinate dimension ($x_D = \cos \alpha$);
α = polar angle from x-axis;
γ_f = unit weight of pore fluid;
η = dimensionless time substitution parameter;
μ = fluid dynamic viscosity;
ν = Poisson's ratio;
ξ = dimensionless time constant; and
τ, τ_D = time integration parameter, dimensionless time integration parameter.